CHAPTER 1

INTRODUCTION

1.1 Materials under Nano regime

1.1.1 Nanomaterials

"There's still plenty of room at the bottom" a quote by the famous theoretical physicist Richard Feynman opened up the era of *"Quantum Dynamics"* involving the unravelling of quantum mechanics in action within extremely small regimes. Thanks to the high-throughput research and development made in the field of energy applications during past few decades which have revolutionized the world with discovery of novel materials possessing unique properties. Amongst the latest cutting-edge fields of nanoscience and nanotechnology, the three major contributing fields are the photovoltaics, optoelectronics and thermoelectrics. Interestingly, the materials from group III-V, like the pnictides of boron, aluminum, gallium and indium, have been studied for all the three applications.[1,2] In addition, precise refinement in the properties of these materials has been achieved by means of chemical doping or by applying external pressure/strain or by imposing dimensional reduction that induces quantum confinement in the material.[3,4] The term quantum confinement relates directly with the word 'nano' (measuring one billionth part of a unit) that is derived from the Greek word ***'nanus'*** meaning *dwarf* had been declared as a standard prefix by General Conference on Weights and Measures (CGPM/GCWM) committee in 1960. A mysterious modulation in the material properties is observed as a result of reduction in its dimension(s)! The dramatic modulation of the material properties (magnitude and trend) depends on the number of reduced/confined dimensions. The zero-, one- and two- dimensional (0D, 1D and 2D) nanostructures have respectively their three, two and one dimensions confined and hence, the transport in those

particular directions is restricted. The effect of dimensional confinement can be validated from the energy dependent responses of the electronic density of states

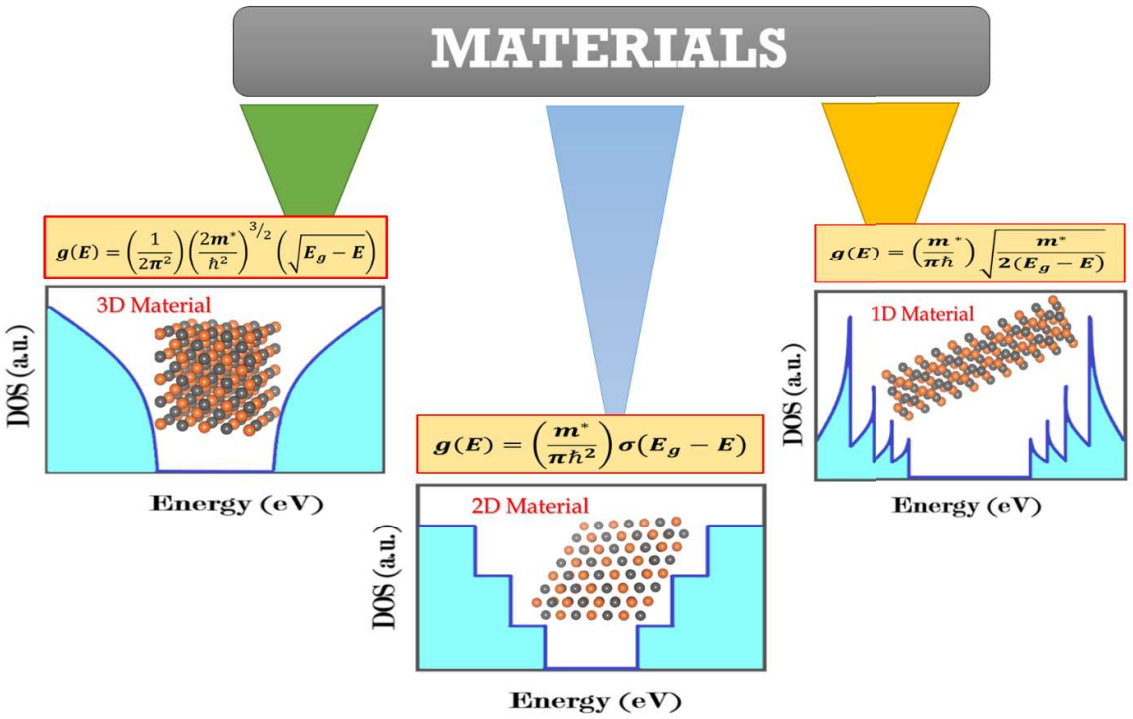

Figure 1.1. Energy dependent responses of electronic density of states (DOS) for bulk, 2D and 1D materials. The crystal structures and DOS equations are embedded with respective systems.

(DOS) of the material (see Fig. 1.1). The evidence of the energy dependent electronic density of states can be validated by the respective equations embedded with respective 3D, 2D and 1D systems. This spatial relation makes the nanomaterials to possess much more interesting electro-optic and transport properties as compared to their bulk counterparts. Since the present thesis deals with nanowires, we shall describe only the nanowire in the following sections.

1.1.2 One-Dimesional Nanomaterials

Amongst the three distinct nanostructures, the two-dimensionally confined one-dimensional (1D) nanostructures like nanotubes, nanoribbons, nano whiskers, nanorods, nanofibers and nanowires (NWs) have drawn great attention of researchers

and materials scientists owing to their versatile properties like strong quantum confinement,[5] carrier trapping[6,7] and moderate electronic bandgap.[8,9] A plethora of research articles that expound the characteristics of growth mechanism,[10] phase engineering[11,12] and heterostructuring (HS)[13,14] of the NWs have emphasized the significance of these 1D systems owing to their versatile nature and multiplicity of application. Further, these 1D systems, especially when constructed by combining the group III and V elements, yield tremendously unexpected results.[15] The literature also reveals the dramatic behaviour of such III-V NWs when subjected to heterostructuring.[16,17] On introducing heterostructured configuration, the existing spatial electronic states can be modulated in a complete controlled manner that ultimately helps in achieving desired transport.[18–21] It should be noted that the introduction heterostructured geometry in NWs may lead to lattice mismatch between the core(bottom) and the shell(top) materials of radial(axial) heterostructure nanowire (HSNW) due to differences in their structural parameters particularly the lattice parameters. The difference in the lattice parameters at the hetero-interface originates due to the diversity of the constituent materials, and therefore, it induces strain within the hetero-layers. Generation of strain within the HSNWs could be considered as one of the factors responsible for trapping/separating the charge carriers or elongating the carrier lifetimes and recombination rates.[22–24] This further helps to understand and tune the mechanism of transport taking place at the hetero-interface.[25] Henceforth, generally for obtaining desired properties with stable configuration, it is expected that the lattice mismatch between the constituent materials of the HS should be minimal or within an acceptable range. More the lattice mismatch, more the strain generated

in the system. Surprisingly, in the case of 1D HSNWs, the generated strain gets released in radial directions therefore, the structural stability of the system becomes achievable with unique interface properties.[25,26] It is interesting to know that despite of being complex in geometry, formation of HSNWs yields such favourable conditions. Experimental reports reveal successful synthesis of radial and axial HSNWs using the vapour-liquid-solid (VLS) method, that facilitates the growth of HSNWs with not only distinct lattice constants of shell and core materials, but also large lattice mismatch with the substrate material.[27–30] The prime reason for the same is the release of strain through the radial directions to the lateral surface of HSNWs. One of the studies on GaAsP/GaP core/shell NW by Himwas et al.[31,32] shows unintentional occurrence of core/shell geometry on deviating the arsenic (As) and phosphorous (P) contents in GaAsP NW. Further, it is observed that without passivation, these NWs do not show significant luminescence; however, on passivating the NW with GaP shell, it induces extra peak in PL spectra, confirming optical transition.[31,32] Zhang et al.[33,34] have suggested strong carrier confinement owing to large differences in the bandgaps of core and shell NWs on combining III-V HSNWs with group-V material shell. The resultant downward surface band bending causes enhancement in the carrier injection efficiency of the system.[35–37]

Keeping the trends of the literature and necessity of filling the gaps between the available data and blanks within the literature, the well-established quantum mechanical tool density functional theory (DFT)[38] (see Fig. 1.2) was utilized for investigating the ground state structural, electronic and optical properties of selected III-V materials under bulk and nano regimes. Further, to modulate the electro-optic

properties of these III-V NWs, the structural manipulations are introduced by means of constructing radial and axial NW heterostructures. To get a deep insight into the underlying mechanism of carrier dynamics within the heterostructured configuration, and to establish a relation between the properties of the system under bulk, NW and HSNW geometries, a comparative assessment of computed properties is carried out. To show significant development and importance of DFT, NWs and heterostructured NWs, the profiles of number of publications versus publication year are represented in Figs. 1.2 (a), (b) and (c), respectively.

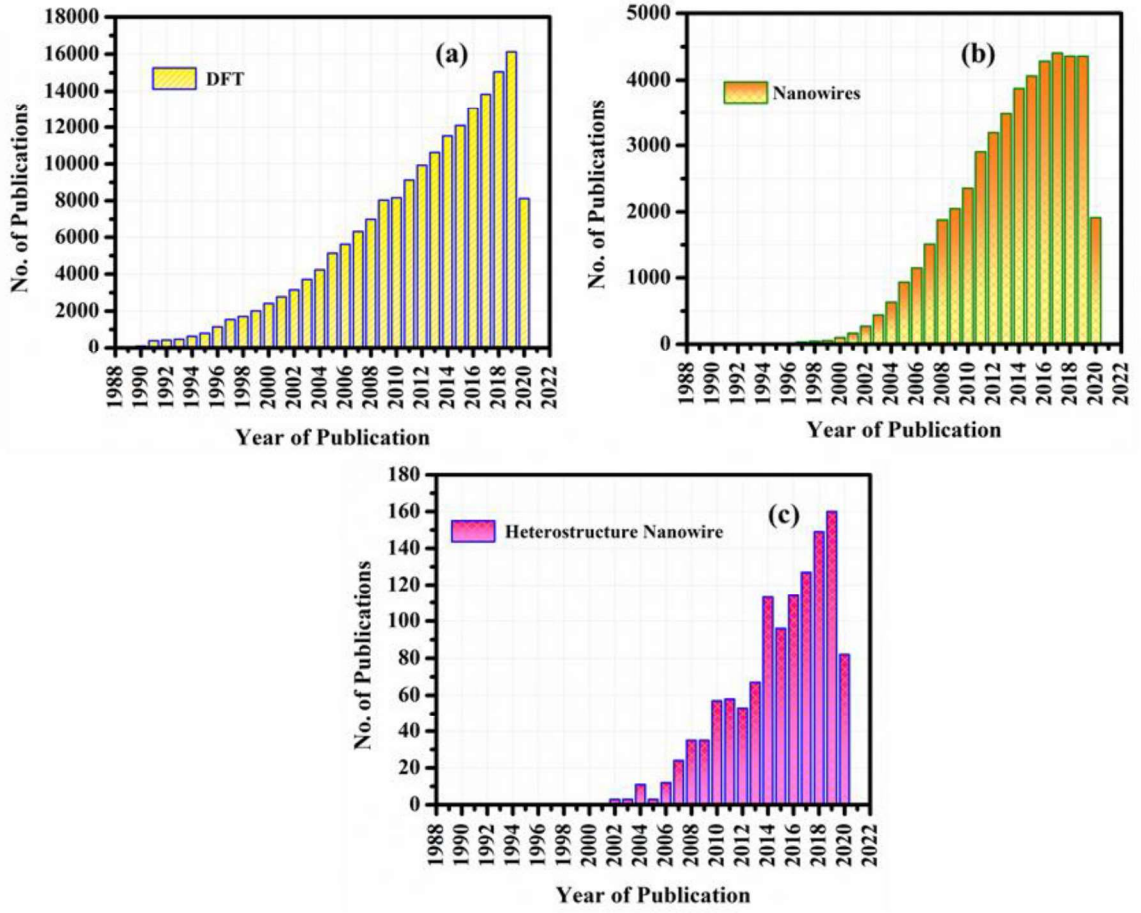

Figure 1.2. Profiles of number of publications versus year of publication is presented for (a) DFT, (b) Nanowires (NWs) and (c) Heterostructure Nanowires (HSNWs) (source: Web of Science as on June-2020).

1.2 Strategies to Improve Properties of Nanowires

Apart from imposing quantum confinement effect, there still remains a few aspects of the system that need tuning according to respective applications. As far as NWs are concerned, the methods that are utilized presently for yielding optimum results from the materials are discussed below:

1.2.1 Tuning Diameter

The assessment of quantum confinement effect can be predicted through dimensional analysis; in the case of NWs, the unique 1D nanomaterials, diameter plays a significant role for defining confinement. Literature survey reveals that the electronic bandgap

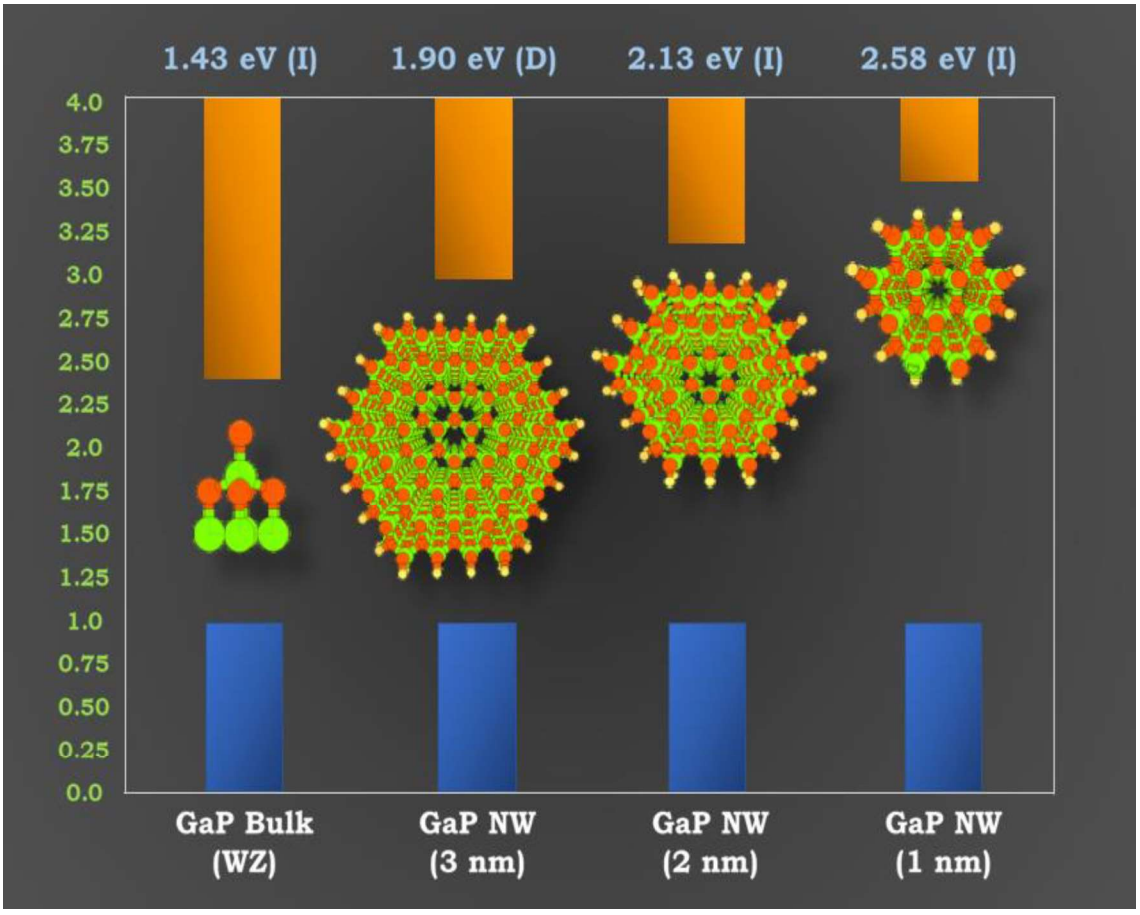

Figure 1.3. Confinement dependent modulation in electronic properties of gallium phosphide (GaP): from bulk to 1D nanowires with three distinct diameters (atoms in green, orange and yellow represent gallium, phosphorous and hydrogen atoms, respectively).

magnitude and dispersion relation are diameter dependent and tailoring indirect to direct bandgap was achieved by means of tuning the NW diameter.[3] It is found that as the diameter of the NW decreases, the electronic bandgap exhibits enhancement and vice-versa.[4] More the diameter of the NW, greater would be its behaviour as a bulk material. Akin to these reports, we have studied the effect of diameter on III-V NW properties. The graphical representation of electronic bandgap alignment with respective bandgap nature and magnitude is represented for gallium phosphide (GaP) (see Fig. 1.3). As it can be clearly observed from the figure, bulk GaP with Wurtzite (WZ) phase possesses indirect bandgap with 1.43 eV magnitude, and on confining the material in form of WZ NW, the gap shows diameter dependent enhancement. Further, the indirect to direct bandgap transition occurs for NW with ~ 3 nm diameter and gap magnitude lying within the optical spectral range. These properties of the GaP NW make it suitable for optoelectronic devices.

1.2.2 External Strain

As discussed earlier, out of three kinds of nanomaterials, NWs that are subjected to spatial confinement in two orthogonal dimensions possess unique properties like quantized and anisotropic conduction.[40] The restricted electronic wave-function then behaves as a unidirectional conducting particle. Unlike diameter tuning, imposing strain on the NW has the advantage of retaining the dimension within feasible range with improved electro-optic transport through the NW.[3,5] As two of the dimensions of the NW are restricted via confinement, there remains only one single dimension with degree of freedom that can be modulated for designing materials with

tailormade properties. This implies that in case of NWs, out of the three distinct types of strains, uniaxial strain is more suitable for tailoring their properties.

1.2.3 Doping/Creation of Defects

Chemical doping refers to the addition of foreign atomic species in the host lattice/material that can modify the intrinsic properties of the material via stoichiometric or composition modulation. The difference between doping and alloying can be assessed by the concentration of the foreign species. In the case of chemical doping, though the concentration is very less, it can dramatically alter the properties of the system; while, the alloy can be viewed as a mixed state of two or more materials that provides an opportunity for overall tuning of the material properties considering multiple aspects. Literature survey reveals the utilization of unique NWs as a photocatalyst for production of hydrogen via water-splitting mechanism.[42,43] Apart from the novel and precious metal-based catalysts, there is a great need for developing metal-free, cost effective and eco-friendly catalyst material. To assess the role of NWs as a catalyst, the adsorption and Gibbs free energy of the selected NWs was computed for pristine and defected conditions, and, the results indicate markable improvement in catalytic activity of the NWs on introduction of substitutional doping.

1.2.4 Constructing Heterostructure

Out of all the listed techniques, researchers have found a unique method of constructing a heterostructure (HS) or heterojunction (HJ) through which fine tuning of the transport properties along a specific direction can be attained. As obvious from the name 'hetero' referring to many or more than one, implying that a combination of

more than one material in the form of 1D or 2D configuration yields a HS. For high-performance field effect transistors (FETs), photovoltaic devices and photocatalysts, it is necessary for a material to possess low carrier recombination rates,[44] which can be achieved by trapping the negative/positive charge carriers in different layers. Trapping of carriers can be done by many means, yet, the heterostructured configuration provides access to the core level conduction mechanism governed by both types of charge carriers thereby providing control over the carrier dynamics. For the successful construction of a HS to be utilized in the latest cutting-edge technologies like photovoltaics, photocatalyst and optoelectronics, there are three major conditions that need to be satisfied[45,46]:

1. There should be as low as possible lattice mismatch between the individual materials contributing to HS formation.
2. The most crucial condition apart from least lattice mismatch is the band offset between the constituent materials, as this solely depends on the position of the electronic edge states of constituent materials.
3. The last but not the least condition to be satisfied is the type-II alignment of the electronic edge states after formation of the HS.

Depending on the position of the electronic edge states of the constituent materials, the band alignments in the HS may give rise to either of the three types of HS namely type-I, type-II or type-III. The schematic diagram representing the typical band alignments in these HSs is shown in Fig. 1.4. As it is clear from the diagram, if the band edge alignment is such as the valence band maxima (VBM) of one heterolayer is higher than the VBM of the other, together with the conduction band minima (CBM)

of the same layer lying at lower energy level than the other one, the HS is of type-I. In case of type-II HS, the VBM and CBM both levels of the second material (B) are lower than the respective VBM and CBM levels of material A. At last, the type-III heterostructure is formed when the VBM and CBM edge states of second materials (B) are aligned lower than the VBM of first material (A), leaving no room for beneficial conduction. Out of all the three types of HSs, the type-II HS is the most desirable one due to its spatially aligned band edge states of heterolayers, that aid very-well in separating the charge carriers through trapping mechanism and improves the overall efficiency of the HS.[7,44] For all devices that enrol the photon induced conduction/transport mechanism need to have type-II HJ/HS configuration for enhanced yield.

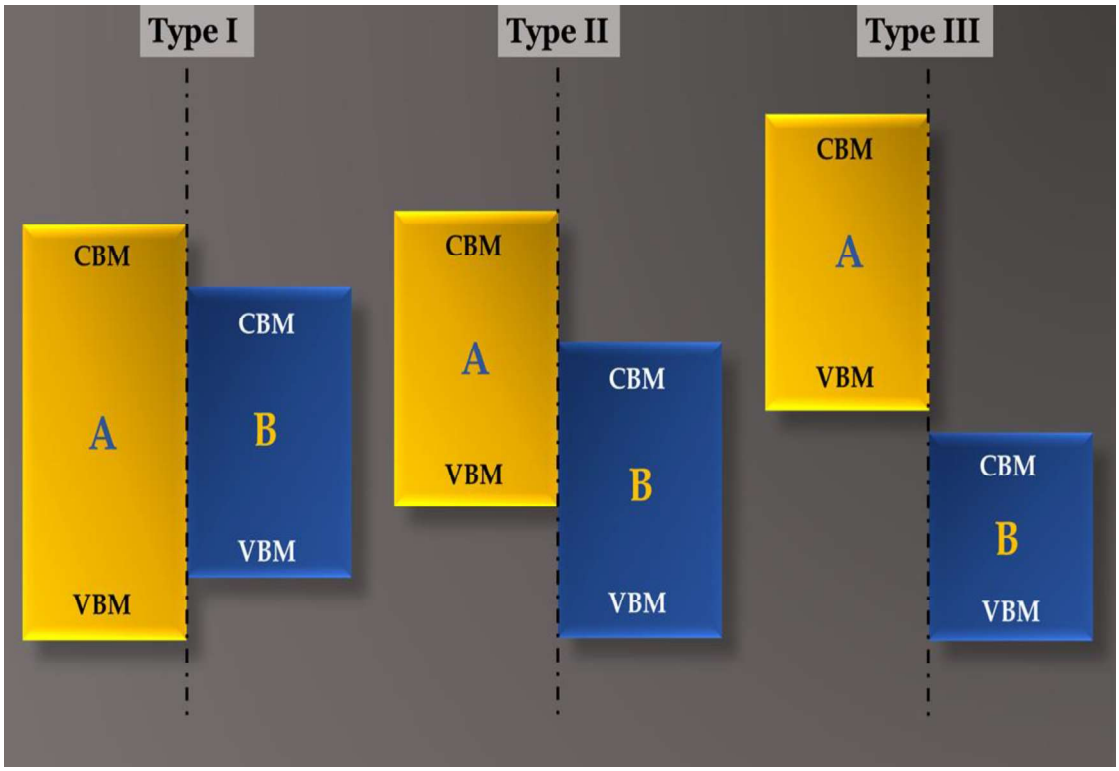

Figure 1.4. **Three distinct types of heterostructures (type-I, type-II and type-III) formed when semiconductor materials (A and B) with different band edge alignments are merged (yellow and blue bars represent the bandgap magnitude of A and B semiconductor materials, respectively.).**

1.3 Research Objectives

The present thesis aims to present the research work carried out on selected bulk and nanostructured III-V compounds under the framework of *first-principles* density functional theory (DFT)[38] for the investigation of their ground state structural, electronic and optical properties. The all forms of III-V compounds have been viewed as the core-materials for cutting-edge technologies like optoelectronics, thermoelectrics and nanoelectronics. Apart from the conventional photovoltaic industry, these materials are also useful for their applicability in the field of photocatalysis for obtaining pure hydrogen from splitting water molecules via solar energy in an eco-friendly and non-hazardous way. One of the major reasons being their desirable range of electronic bandgaps that fall in the visible range of electro-magnetic spectrum with direct type of nature. The other reason being their metal free crystal structures with wide range of tuneable properties together with chemical and physical robustness. The specific objectives of the present thesis are listed below:

1. To compute the structural, electronic, optical and thermoelectric properties of selected III-V compounds with their polytypic bulk phases.
2. To construct two-dimensionally confined NWs from the optimized bulk unit cells of the selected III-V compounds, and investigate their structural, electronic, and optical properties.
3. To construct the axial/radial heterostructure nanowires (HSNWs).
4. To compute the structural, electronic and optical properties of the HSNWs and establish a relationship between the size, shape, material and phase dependent properties of the HSNWs for building a pathway for designing unique

materials with desired properties such as electronic, optoelectronic, catalytic and thermoelectric.

1.4 Structure of the Thesis

After the achievement of the aforementioned objectives, we have integrated the results with respective discussions in six different chapters.

CHAPTER 1 presents a brief description of the contribution of the III-V materials in the fields of optoelectronics, nanoelectronics and thermoelectrics and the advancements made in these group of materials through chemical doping or through modifying the structural phase and/or imposing strain/confinement, etc. The different III-V materials like gallium nitride, gallium phosphide, gallium arsenide, gallium antimonide, boron nitride, boron phosphide, boron arsenide, etc. have significantly contributed to the field of optoelectronics to thermoelectric devices; especially, the group III-nitrides and -arsenides have become famous owing to their adaptable electro-optic transport characteristic profiles. One of the reports on GaP NWs grown with Wurtzite phase suggests direct nature of electronic bandgap with magnitude 2.17 eV in contrast to its bulk counterpart.[47,48] This gap, being direct in nature, suggests its utilization in optoelectronic devices. Apart from the III-nitrides and -arsenides, the gallium antimonide based HSNWs have received scarce attention, and need to be explored owing to their high thermoelectric figure of merit in its bulk phase,[48] which can be enhanced by means of dimensional confinement.[49] Apart from gallium based HSNWs, the aluminium based pristine HSNWs have not been studied so far for testing their application in the fields of optoelectronics and photovoltaics.

CHAPTER 2 covers the step-by-step description regarding the theoretical aspects and computational approach utilized for studying the proposed properties of selected III-V materials under bulk and nano regimes. The first theoretical approach starting from Born-Oppenheimer approximation to the latest ground breaking electron density-based approximation formulated by Walter Kohn and Lu Jeu Sham together with different exchange-correlation functionals based on local density approximation (LDA) and generalized gradient approximation (GGA) for the construction of pseudopotentials are systematically described. Apart from the electronic properties, we have also evaluated the optical, vibrational and thermoelectric properties of the proposed systems and, respective approaches have been included in this chapter. The evaluation of optical transport properties has been done by computing the frequency dependent complex di-electric function of the materials that explicitly gives graphical representation of the optical transport as a function of photon energy thus, validating the active regime of the material within the electro-magnetic spectrum. To validate the stability of the materials and to unravel the phonon dynamics of the material, the density functional perturbation theory (DFPT)[50] has been applied. Last but not the least, the present chapter sheds light on the deformation potential theory utilized in conjunction with the Boltzmann Transport theory utilized for evaluating electron and phonon contributions to the overall thermoelectric transport properties of the materials.

CHAPTER 3 is focused on the structural, electronic, vibrational and thermoelectric properties of the gallium pnictides, GaX (X=P, As, Sb) taking into consideration the two polytypic phases, the cubic zinc blende (ZB) and the hexagonal wurtzite (WZ).

The electronic band structure calculation performed for all systems reveals direct nature of electronic bandgap except for GaP. Encouraged by the moderate and direct nature of the electronic bandgap of these materials, and to validate their applicability to the field of thermoelectrics, the vibrational dynamics of the systems was evaluated by means of computing the phonon dispersion curves (PDCs) and phonon density of states (PHDOS). The absence of soft phonon modes and/or imaginary frequency components in the PDCs of all the systems validates the dynamic stability of the systems in both polytypic phases. The PHDOSs were utilized for assessing the thermal transport properties of the systems and, the 2^{nd} order inter-atomic harmonic force constants (IFCs) were utilized for computing the 3^{rd} order anharmonic IFCs that can be further used for solving the Boltzmann transport equations (BTE) for phonons that account for assessing phonon contributions to thermoelectric properties. At the end, the results on phase dependent thermoelectric properties of GaX systems show that the WZ phase, the most preferred phase at nanoscale, gives lower thermal conductivity and higher thermoelectric figure of merit (ZT) which indicate the thermoelectric efficiency of the material. Furthermore, the GaSb stands out as a promising candidate for thermoelectric applications amongst the remaining pnictide siblings. After getting markable results on the electronic, vibrational and thermoelectric profiles of GaX compounds in WZ phase, two-dimensionally confined 1D nanostructures were constructed for understanding the modification in the properties of GaX subjected to size-effect. As expected, the strong quantum confinement effect resulted in expansion of the band edge states of all the three systems. To get a deep insight into the properties of these NWs, all the computations

were reperformed by varying the size (diameter (~1, 2 and 3 nm)) of the NWs and by applying uniaxial external strain. These two parameters also help in tuning the properties of the NWs according to the desired application. The diameter dependent profiles of the electro-optic properties of GaX NWs suggest that the GaP NW with ~3 nm diameter shows direct nature of electronic band gap with moderate magnitude of 1.90 eV, whereas, the remaining sibling NWs retain indirect nature of bandgap with reduction in gap magnitude as a function of NW diameter (2.27, 1.86 and 1.60 eV for GaAs NW and 1.68, 1.25 and 0.99 eV for GaSb NW, respectively). The results of strain dependent electronic responses of the NWs reveal dramatic indirect to direct bandgap transition for GaAs and GaSb NWs at 4% uniaxial compressive strain, whereas for GaP NW, the threshold value for such transition is 2%. Furthermore, the frequency dependent complex di-electric functions are evaluated; which suggests that peak absorption of electro-magnetic energy occurs within visible-ultraviolet region. Owing to these observations, the applicability of these systems can be evaluated in the field of optoelectronic and photovoltaic devices. On the other hand, the dramatic indirect to direct electronic transition observed at 4% for GaAs and GaSb NW (2% for GaP NW) uniaxial compressive strain suggests that these NWs can be utilized in strain mediated switching devices. The unique electro-optic and vibrational responses of the systems provide inspiration for studying the system for thermoelectric applications.

Moving towards the main objective of the present research work, the optimized pristine GaX NWs were utilized for constructing the radial heterostructures (HSs) with core/shell (CS) geometry. The two such core/shell HSNWs namely, GaSb/GaP and GaSb/GaAs, were constructed and respective electro-optic responses were

evaluated under the approach described in **CHAPTER 2** and the corresponding results are presented in the next chapter, **CHAPTER 4**. To study the effect of shape dependent modifications in the HSNW properties, the shell NWs made up of GaP and GaAs NWs were embedded on the GaSb core NWs constructed with two distinct cross-sectional areas (round (R) and triangular (T)). The overall cross-section of all the HSNWs were kept to be hexagonal. The first-time studied approach of tailoring the system properties with respect to core shape and shell materials could be a unique pathway for tuning the electro-optic transport through the HSNWs. This also gives opportunity to precisely modulate the charge carrier recombination rates through surface charge trapping, subjected to distinct electronic edge states of the hetero-layers (core/shell). The best way to assess the cause of the modulation in the transport and the edge states, is to evaluate the conduction and valence band edge states of the hetero-layers and investigate the band alignment subjected to heterostructured geometry of the NWs. Depending on the band alignment, there are three types of heterostructures, namely, type-I, type-II and type-III. Amongst the three types, type-II heterostructure is the most preferable configuration owing to its ability to trap surface charge carriers and decrease the recombination rates. This unique characteristic is the foundation for the construction of opto-electronic devices and photovoltaic solar cells. Following this, we have computed the solar cell parameters of the HSNWs and compared them with the pristine GaX (X=P, As, Sb) NWs. The results show that the pristine GaSb NW with ~ 2nm diameter possesses highest power conversion efficiency of 32% amongst all considered systems. Apart from the pristine

NWs, the GaSb-GaAs HSNWs possess markable efficiency of 16% which suggest that the HSNWs could be the suitable candidates for photovoltaic devices.

Being the most contributing materials, besides GaX compounds, we have also considered two famous aluminium based pnictide compounds namely, aluminum phosphide (AlP) and aluminum arsenide (AlAs) for computation, and, for inspecting their structural, electronic and optical properties under bulk and confined geometries. The respective results of the considered materials are presented in **CHAPTER 5**. These two compounds have been reported for their markable performance and have been utilized for optoelectronics to photovoltaics.[2] Similar to the other III-V compounds, AlP and AlAs also tend to crystallize in WZ phase with hexagonal symmetry under confined geometry, despite existing in ZB phase with cubic symmetry in their bulk counterpart. To systematically study the phase dependent properties of these materials, the bulk AlP and AlAs were first studied under the proposed approach and then the optimized unit cells of both compounds were considered for the construction of the pristine AlP and AlAs NWs. Structural, electronic and optical transport properties were computed for both NWs for the assessment of quantum confinement effect. Dramatic indirect to direct band gap transition in the case of AlP compound was observed subjected to two-dimensional confinement; whereas, the AlAs preserves its indirect nature of electronic bandgap even after imposing confinement. As expected, the dimensional confinement of both compounds results in enhancement of the electronic band gap magnitude. These results indicate that the AlP under confined dimensions is suitable for optoelectronic applications owing to its direct and moderate magnitude of bandgap. The next step in the study was to utilize these

pristine NWs for constructing the axial and radial HSNWs. The two variants of radial HSNWs AlP/AlAs and AlAs/AlP were then considered for fully optimizing all the structural parameters under specific threshold criteria. The electronic and optical transport properties of the core/shell heterostructure NWs (CS-HSNWs) unravel spatially confined charge carriers owing to the desired band gap alignment. The bandgap magnitude of 2.72 eV with direct nature in the case of AlAs/AlP CS-HSNW supports the applicability of the considered HSNW in the field of photovoltaic solar cells as the high-energy photon absorber layer. On the other hand, the second variant AlP/AlAs CS-HSNW with indirect nature shows less suitability in optical devices. Apart from the band alignment, the electronic band structure calculations reveal indirect nature of the bandgap with gap magnitude of 2.60 eV in the latter case. Inspired by these results and to explore geometry dependence, the axial HSNW (A-HSNW) from AlP and AlAs NWs was then constructed by stacking the individual unit cells of the pristine NWs on each other along 0001 direction. This constructed axial HSNW was then fully relaxed till the convergence criteria were not achieved. All proposed properties evaluated for bulk, pristine NWs and CS-HSNWs were then computed for the AlP/AlAs A-HSNW. This chapter provides full-insight into the electro-optic transport properties of AlX compounds ranging from their bulk phase to the confined NW geometry to the spatially constructed radial and axial HSNW configurations, and also sheds light on unique pathways to engineering the carrier dynamics in the semiconducting NWs.

The last chapter of the thesis, **CHAPTER 6** contains the results and discussion on the applicability of the group III-based phosphide NWs in one of the emerging energy

application fields, i.e. hydrogen generation through water-splitting process by computing the hydrogen evolution reaction (HER) and oxygen evolution reaction (OER) based catalytic activity of the systems. The results of electronic properties suggest indirect to direct bandgap transition of the systems under quantum size effect with enhancement in gap magnitude. Furthermore, to finely tune the properties, the NWs were subjected to substitutional defect/doping, and it is observed that the chemically modified NWs are more sensitive to hydrogen/oxygen adsorption and yield pronounced catalytic activities. The obtained results show significance of metal-free novel materials that have potential to be utilized as active HER/OER catalysts because of their unique properties. Although the III-V compounds not being extremely abundant, yet under confined geometry they provide a scope for their utility owing to the reduced need of material and admirable responses. We believe that further enhancement in the catalytic response of the NWs can be achieved by means of tailoring the electronic bandgap of the system(s) via optimizing the dopant concentration and/or phase or structure engineering.

The overall conclusion based on the results on the structural, electronic, optical, vibrational and thermoelectric properties of the considered III-V compounds ranging from their bulk phase to nanostructured complex geometries are summarized in **CHAPTER 7**. Both the groups; i.e. GaX(X=P, As, Sb) and AlX (X=P, As) standout as the suitable candidates for optoelectronic and photovoltaic nano-device based applications. The dramatic effects of nanostructuring and heterostructuring has been observed in both cases. Further enhancement in electro-optic responses of the pristine NWs has been made by introducing radial and axial heterostructured configurations.

We believe, that the results shed light to the pathway for engineering the properties of the system by means of engineering the phase, dopant concentration, size, shape, geometry and composition. At the end, the thesis details a brief description on the scope of probable future research avenues.

References

(1) Han, J.; Amano, H.; Schowalter, L. Deep UV LEDs. *Semicond. Sci. Technol.* **2014**, *29* (8), 080301. https://doi.org/10.1088/0268-1242/29/8/080301

(2) Boras, G.; Yu, X.; Liu, H. III-V Ternary Nanowires on Si Substrates: Growth, Characterization and Device Applications. *J. Semicond.* **2019**, *40* (10), 101301. https://doi.org/10.1088/1674-4926/40/10/101301

(3) Dabhi, S. D.; Jha, P. K. Ab Initio Study of Strained Wurtzite InAs Nanowires: Engineering an Indirect-Direct Band Gap Transition through Size and Uniaxial Strain. *RSC Adv.* **2015**, *5* (109), 89993–90000. https://doi.org/10.1039/c5ra16512a

(4) Galicka, M.; Buczko, R.; Kacman, P.; Lima, E. N.; Schmidt, T. M.; Shtrikman, H. First Principles Studies of Structural, Electrical and Magnetic Properties of Semiconductor Nanowires. *Phys. Status Solidi - Rapid Res. Lett.* **2013**, *7* (10), 739–753. https://doi.org/10.1002/pssr.201307234

(5) Wu, Z.; Neaton, J. B.; Grossman, J. C. Quantum Confinement and Electronic Properties of Tapered Silicon Nanowires. *Phys. Rev. Lett.* **2008**, *100* (24), 236805. https://doi.org/10.1103/PhysRevLett.100.246804

(6) Johnson, J. C.; Knutsen, K. P.; Yan, H.; Law, M.; Zhang, Y.; Yang, P.; Saykally, R. J. Ultrafast Carrier Dynamics in Single ZnO Nanowire and Nanoribbon Lasers. *Nano Lett.* **2004**, *4* (2), 197–204. https://doi.org/10.1021/nl034780w

(7) Lo, S. S.; Major, T. A.; Petchsang, N.; Huang, L.; Kuno, M. K.; Hartland, G. V. Charge Carrier Trapping and Acoustic Phonon Modes in Single CdTe Nanowires. *ACS Nano* **2012**, *6* (6), 5274–5282. https://doi.org/10.1021/nn3010526

(8) Li, Y.; Qian, F.; Xiang, J.; Lieber, C. M. Nanowire Electronic and Optoelectronic Devices. *Mater. Today* **2006**, *9* (10), 18–27. https://doi.org/10.1016/S1369-7021(06)71650-9

(9) Nolan, M.; O'Callaghan, S.; Fagas, G.; Greer, J. C.; Frauenheim, T. Silicon Nanowire Band Gap Modification. *Nano Lett.* **2007**, *7* (1), 34–38. https://doi.org/10.1021/nl061888d

(10) Tersoff, J. Stable Self-Catalyzed Growth of III-V Nanowires. *Nano Lett.* **2015**, *15* (10), 6609–6613. https://doi.org/10.1021/acs.nanolett.5b02386

(11) Meister, S.; Peng, H.; McIlwrath, K.; Jarausch, K.; Zhang, X. F.; Cui, Y. Synthesis and

Characterization of Phase-Change Nanowires. *Nano Lett.* **2006**, *6* (7), 1514–1517. https://doi.org/10.1021/nl061102b

(12) Dick, K. A.; Thelander, C.; Samuelson, L.; Caroff, P. Crystal Phase Engineering in Single InAs Nanowires. *Nano Lett.* **2010**, *10* (9), 3494–3499. https://doi.org/10.1021/nl101632a

(13) Qian, F.; Li, Y.; Gradečak, S.; Wang, D.; Barrelet, C. J.; Lieber, C. M. Gallium Nitride-Based Nanowire Radial Heterostructures for Nanophotonics. *Nano Lett.* **2004**, *4* (10), 1975–1979. https://doi.org/10.1021/nl0487774

(14) Wu, Y.; Xiang, J.; Yang, C.; Lu, W.; Lieber, C. M. Single-Crystal Metallic Nanowires and Metal/Semiconductor Nanowire Heterostructures. *Nature* **2004**, *430* (6995), 61–65. https://doi.org/10.1038/nature02674

(15) Samuelson, L.; Thelander, C.; Björk, M. T.; Borgström, M.; Deppert, K.; Dick, K. A.; Hansen, A. E.; Mårtensson, T.; Panev, N.; Persson, A. I.; et al. Semiconductor Nanowires for OD and ID Physics and Applications. *Phys. E Low-Dimensional Syst. Nanostructures* **2004**, *25* (2-3 SPEC.ISS.), 313–318. https://doi.org/10.1016/j.physe.2004.06.030

(16) Joyce, H. J.; Gao, Q.; Tan, H. H.; Jagadish, C.; Kim, Y.; Fickenscher, M. A.; Perera, S.; Hoang, T. B.; Smith, L. M.; Jackson, H. E.; et al. Unexpected Benefits of Rapid Growth Rate for III−V Nanowires. *Nano Lett.* **2009**, *9* (2), 695–701. https://doi.org/10.1021/nl803182c

(17) Lim, S. K.; Brewster, M.; Qian, F.; Li, Y.; Lieber, C. M.; Gradečak, S. Direct Correlation between Structural and Optical Properties of III - V Nitride Nanowire Heterostructures with Nanoscale Resolution. *Nano Lett.* **2009**, *9* (11), 3940–3944. https://doi.org/10.1021/nl9025743

(18) Jiang, X.; Xiong, Q.; Nam, S.; Qian, F.; Li, Y.; Lieber, C. M. InAs/InP Radial Nanowire Heterostructures as High Electron Mobility Devices. *Nano Lett.* **2007**, *7* (10), 3214–3218. https://doi.org/10.1021/nl072024a

(19) Hu, Y.; Churchill, H. O. H.; Reilly, D. J.; Xiang, J.; Lieber, C. M.; Marcus, C. M. A Ge/Si Heterostructure Nanowire-Based Double Quantum Dot with Integrated Charge Sensor. *Nat. Nanotechnol.* **2007**, *2* (10), 622–625. https://doi.org/10.1038/nnano.2007.302

(20) Songmuang, R.; Katsaros, G.; Monroy, E.; Spathis, P.; Bougerol, C.; Mongillo, M.; De Franceschi, S. Quantum Transport in GaN/AlN Double-Barrier Heterostructure Nanowires. *Nano Lett.* **2010**, *10* (9), 3545–3550. https://doi.org/10.1021/nl1017578

(21) Xiang, J.; Lu, W.; Hu, Y.; Wu, Y.; Yan, H.; Lieber, C. M. Ge/Si Nanowire Heterostructures as High-Performance Field-Effect Transistors. *Nature* **2006**, *441* (7092), 489–493. https://doi.org/10.1038/nature04796

(22) Parkinson, P.; Joyce, H. J.; Gao, Q.; Tan, H. H.; Zhang, X.; Zou, J.; Jagadish, C.; Herz, L. M.; Johnston, M. B. Carrier Lifetime and Mobility Enhancement in Nearly Defect-Free Core-Shell Nanowires Measured Using Time-Resolved Terahertz Spectroscopy. *Nano Lett.* **2009**, *9* (9), 3349–3353. https://doi.org/10.1021/nl9016336

(23) Guo, W.; Zhang, M.; Bhattacharya, P.; Heo, J. Auger Recombination in III-Nitride Nanowires and Its Effect on Nanowire Light-Emitting Diode Characteristics. *Nano Lett.* **2011**, *11* (4), 1434–1438. https://doi.org/10.1021/nl103649d

(24) Joyce, H. J.; Wong-Leung, J.; Yong, C. K.; Docherty, C. J.; Paiman, S.; Gao, Q.; Tan, H. H.; Jagadish, C.; Lloyd-Hughes, J.; Herz, L. M.; et al. Ultralow Surface Recombination Velocity in InP Nanowires Probed by Terahertz Spectroscopy. *Nano Lett.* **2012**, *12* (10), 5325–5330. https://doi.org/10.1021/nl3026828

(25) Osadchiĭ, V. M.; Prinz, V. Y. Charge-Carrier Separation in Rolled Heterostructures. *JETP Lett.* **2000**, *72* (6), 312–315. https://doi.org/10.1134/1.1328445

(26) Yan, X.; Fan, S.; Zhang, X.; Ren, X. Analysis of Critical Dimensions for Nanowire Core-Multishell Heterostructures. *Nanoscale Res. Lett.* **2015**, *10* (1), 1–7. https://doi.org/10.1186/s11671-015-1097-7

(27) Caroff, P.; Messing, M. E.; Mattias Borg, B.; Dick, K. A.; Deppert, K.; Wernersson, L. E. InSb Heterostructure Nanowires: MOVPE Growth under Extreme Lattice Mismatch. *Nanotechnology* **2009**, *20* (49), 495606. https://doi.org/10.1088/0957-4484/20/49/495606

(28) Cirlin, G. E.; Dubrovskii, V. G.; Soshnikov, I. P.; Sibirev, N. V.; Samsonenko, Y. B.; Bouravleuv, A. D.; Harmand, J. C.; Glas, F. Critical Diameters and Temperature Domains for MBE Growth of III-V Nanowires on Lattice Mismatched Substrates. *Phys. Status Solidi - Rapid Res. Lett.* **2009**, *3* (4), 112–114. https://doi.org/10.1002/pssr.200903057

(29) Kavanagh, K. L. Misfit Dislocations in Nanowire Heterostructures. *Semicond. Sci. Technol.* **2010**, *25* (2), 024006. https://doi.org/10.1088/0268-1242/25/2/024006

(30) Fröberg, L. E.; Wacaser, B. A.; Wagner, J. B.; Jeppesen, S.; Ohlsson, B. J.; Deppert, K.; Samuelson, L. Transients in the Formation of Nanowire Heterostructures. *Nano Lett.* **2008**, *8* (11), 3815–3818. https://doi.org/10.1021/nl802149v

(31) Himwas, C.; Collin, S.; Chen, H. L.; Patriarche, G.; Oehler, F.; Travers, L.; Saket, O.; Julien, F. H.; Harmand, J. C.; Tchernycheva, M. Correlated Optical and Structural Analyses of Individual GaAsP/GaP Core-Shell Nanowires. *Nanotechnology* **2019**, *30* (30), 304001. https://doi.org/10.1088/1361-6528/ab1760

(32) Himwas, C.; Collin, S.; Rale, P.; Chauvin, N.; Patriarche, G.; Oehler, F.; Julien, F. H.; Travers, L.; Harmand, J. C.; Tchernycheva, M. In Situ Passivation of GaAsP Nanowires. *Nanotechnology* **2017**, *28* (49), 495707. https://doi.org/10.1088/1361-6528/aa9533

(33) Zhang, S.; Connie, A. T.; Laleyan, D. A.; Nguyen, H. P. T.; Wang, Q.; Song, J.; Shih, I.; Mi, Z. On the Carrier Injection Efficiency and Thermal Property of InGaN/GaN Axial Nanowire Light Emitting Diodes. *IEEE J. Quantum Electron.* **2014**, *50* (6), 483–490. https://doi.org/10.1109/JQE.2014.2317732

(34) Zhang, Y.; Aagesen, M.; Holm, J. V.; Jørgensen, H. I.; Wu, J.; Liu, H. Self-Catalyzed GaAsP Nanowires Grown on Silicon Substrates by Solid-Source Molecular Beam Epitaxy. *Nano Lett.* **2013**, *13* (8), 3897–3902. https://doi.org/10.1021/nl401981u

(35) Nguyen, H. P. T.; Zhang, S.; Connie, A. T.; Kibria, M. G.; Wang, Q.; Shih, I.; Mi, Z. Breaking the Carrier Injection Bottleneck of Phosphor-Free Nanowire White Light-Emitting Diodes. *Nano Lett.* **2013**, *13* (11), 5437–5442. https://doi.org/10.1021/nl4030165

(36) Barrigón, E.; Heurlin, M.; Bi, Z.; Monemar, B.; Samuelson, L. Synthesis and Applications of III-V Nanowires. *Chem. Rev.* **2019**, *119* (15), 9170–9220. https://doi.org/10.1021/acs.chemrev.9b00075

(37) Hyun, J. K.; Zhang, S.; Lauhon, L. J. Nanowire Heterostructures. *Annu. Rev. Mater. Res.* **2013**, *43* (1), 451–479. https://doi.org/10.1146/annurev-matsci-071312-121659

(38) Kohn, W.; Sham, L. J. Self-Consistent Equations Including Exchange and Correlation Effects. *Phys. Rev.* **1965**, *140* (4A), A1133. https://doi.org/10.1103/PhysRev.140.A1133

(39) Copple, A.; Ralston, N.; Peng, X. Engineering Direct-Indirect Band Gap Transition in Wurtzite GaAs Nanowires through Size and Uniaxial Strain. *Appl. Phys. Lett.* **2012**, *100* (19), 193108. https://doi.org/10.1063/1.4718026

(40) Mohammad, N. S. Understanding Quantum Confinement in Nanowires: Basics, Applications and Possible Laws. *J. Phys. Condens. Matter* **2014**, *26* (42), 423202. https://doi.org/10.1088/0953-8984/26/42/423202

(41) Peng, X.; Copple, A. Origination of the Direct-Indirect Band Gap Transition in Strained Wurtzite and Zinc-Blende GaAs Nanowires: A First Principles Study. *Phys. Rev. B - Condens. Matter Mater. Phys.* **2013**, *87* (11), 115308. https://doi.org/10.1103/PhysRevB.87.115308

(42) Wang, G.; Wang, H.; Ling, Y.; Tang, Y.; Yang, X.; Fitzmorris, R. C.; Wang, C.; Zhang, J. Z.; Li, Y. Hydrogen-Treated TiO2 Nanowire Arrays for Photoelectrochemical Water Splitting. *Nano Lett.* **2011**, *11* (7), 3026–3033. https://doi.org/10.1021/nl201766h

(43) Ismail, A. A.; Bahnemann, D. W. Photochemical Splitting of Water for Hydrogen Production by Photocatalysis: A Review. *Sol. Energy Mater. Sol. Cells* **2014**, *128*, 85–101. https://doi.org/10.1016/j.solmat.2014.04.037

(44) Dai, X.; Zhang, S.; Wang, Z.; Adamo, G.; Liu, H.; Huang, Y.; Couteau, C.; Soci, C. GaAs/AlGaAs Nanowire Photodetector. *Nano Lett.* **2014**, *14* (5), 2688–2693. https://doi.org/10.1021/nl5006004

(45) Chen, J.; Ma, Q.; Wu, X. J.; Li, L.; Liu, J.; Zhang, H. Wet-Chemical Synthesis and Applications of Semiconductor Nanomaterial-Based Epitaxial Heterostructures. *Nano-Micro Lett.* **2019**, *11* (1), 86. https://doi.org/10.1007/s40820-019-0317-6

(46) Alferov, Z. I. The Double Heterostructure: Concept and Its Applications in Physics, Electronics and Technology. *Int. J. Mod. Phys. B* **2002**, *16* (5), 647–675. https://doi.org/10.1142/S0217979202010233

(47) Assali, S.; Zardo, I.; Plissard, S.; Kriegner, D.; Verheijen, M. A.; Bauer, G.; Meijerink, A.; Belabbes, A.; Bechstedt, F.; Haverkort, J. E. M.; et al. Direct Band Gap Wurtzite Gallium Phosphide Nanowires. *Nano Lett.* **2013**, *13* (4), 1559–1563.

https://doi.org/10.1021/nl304723c

(48) Gajaria, T. K.; Dabhi, S. D.; Jha, P. K. Ab Initio Energetics and Thermoelectric Profiles of Gallium Pnictide Polytypes. *Sci. Rep.* **2019**, *9* (1), 5884. https://doi.org/10.1038/s41598-019-41982-9

(49) Mingo, N. Thermoelectric Figure of Merit and Maximum Power Factor in III-V Semiconductor Nanowires. *Appl. Phys. Lett.* **2004**, *84* (14), 2652–2654. https://doi.org/10.1063/1.1695629

(50) Baroni, S.; De Gironcoli, S.; Dal Corso, A.; Giannozzi, P. Phonons and Related Crystal Properties from Density-Functional Perturbation Theory. *Reviews of Modern Physics*. April **2001**, *73*, 515–562. https://doi.org/10.1103/RevModPhys.73.515
